Coupled Mechanical-Electrical Modeling of the TARSIS Experiment

A. Torre, D. Ciazynski, D. Durville, H. Bajas, and A. Nijhuis

***Abstract*—Nb_3Sn is now commonly used in the design of high-field large-scale magnets. However, it is a brittle material, the superconducting properties of which degrade under mechanical strain. Both ITER TF and CS magnets make use of Nb_3Sn strands in cable-in-conduit conductors. Experiments have been carried out in the TARSIS facility at University of Twente aiming at measuring the strand critical current as a function of periodically applied strain/stress. Until recently, these experiments have given good indications of the strand behavior, but they had not been fully understood because of the lack of an accurate description of the local strain along the tested strand. Furthermore, they cannot be extrapolated directly to a real cable-in-conduit conductor because they do not simulate the differential thermal contraction, which puts the strand under longitudinal compression. Using the mechanical code MULTIFIL developed at Ecole Centrale de Paris, associated with the electrical code CARMEN developed at CEA/IRFM, this paper aims at understanding the mechanisms of the critical current reduction during a TARSIS experiment by coupling the local strain map of the strand to the complex current paths between Nb_3Sn filaments. Comparison with experimental results and with analytic limiting cases are presented and discussed.**

***Index Terms*—Mechanical properties, modeling, Nb_3Sn strands, strain dependence.**

I. Introduction

In superconducting cable in conduit conductors (CICC), strands are subject to high mechanical loading due to both thermal contraction of the steel jacket and electromagnetic load. The strain dependence of Nb_3Sn-based strands performances, along with the complex strain map induced by the CIC cabling pattern make it very difficult to predict reliably any cable's performances. Although the test of the ITER TF in the SULTAN facility has led to the acceptance of all conductors, it has also shown that not only initial performances could be lower than expected, but also that cycling would degrade these CCICs even more, as observed in [1]–[3]. If the Nb_3Sn sensitivity to strain has been identified as the main driver of this degradation, there is still no clear explanation of this phenomenon. In order to understand better the strand behavior, this article proposes to compare experimental data from an ITER-type strand measurement campaign with the results of a mechanical-electrical model.

Manuscript received October 9, 2012; accepted January 23, 2013. Date of publication January 29, 2013; date of current version April 10, 2013. This work was supported in part by the ITER Contract CT/09/4300000014.

A. Torre and D. Ciazynski are with the Cryomagnetism Group, Comissariat à l'Énergie Atomique-Cadarache, St-paul Lez Durance 13108, France (e-mail: alexandre.torre@cea.fr; daniel.ciazynski@cea.fr).

D. Durville is with the Soil, Structure and Materials Mechanics Laboratory, École Centrale de Paris, F-92 295 Châtenay-Malabry Cedex, France (e-mail: damien.durville@ecp.fr).

H. Bajas is with the Technology Department, CERN, 1211 CH, Geneva 23, Switzerland (e-mail: hugues.bajas@cern.ch).

A. Nijhuis is with the Faculty of Science and Technology, Twente University, 7500 AE Enschede, The Netherlands (e-mail: a.nijhuis@tnw.utwente.nl).

Color versions of one or more of the figures in this paper are available online at http://ieeexplore.ieee.org.

Digital Object Identifier 10.1109/TASC.2013.2243494

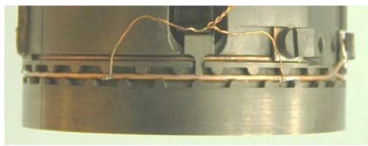

Fig. 1. TARSIS periodic bending probe.

II. The TARSIS Experiment

A. Description

TARSIS is one of the only tests that aim at understanding the strand behavior under mechanical load, in this case a periodic bending load simulating the electromagnetic loading in a cable, and that has been performed on a large number of superconducting strands. In particular, ITER TF and CS strands were extensively tested. The experiment consists in measuring the V(I) characteristic of the strand, at 4.2 K and 12 T, while applying an increasing periodic bending load of period L_{T}. It is described in detail in [4] (Fig. 1).

This experiment is all the more important that the usual scaling laws describing the $I_{\mathrm{C}}(B, T, \varepsilon)$ relation do not take into account any possible variation of I_{C} with a non-uniform strain in the cross-section of the strand.

B. Strand Studied and TARSIS Results

The strand chosen for this study is a Bronze Route ITER-type TF strand of diameter 0.82 mm, with a filamentary radius $r_{\mathrm{zf}} = 0.274$ mm and a filament twist pitch $Lp = 15$ mm.

Fig. 2 shows the scaling law of the strand along with experimental measurement. TARSIS results give the I_{C} and n-value of the strand with respect to the applied load F (N/m) or probe deflection D (μm), both measured during the experiment.

III. MULTIFIL Mechanical Model

A. Description of the Model

The MULTIFIL code, developed at Ecole Centrale de Paris (ECP) is a finite element code that allows solving the mechanical equilibrium of one or several strands under loading conditions. It has been used extensively to describe ITER

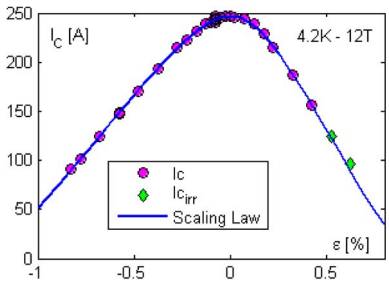

Fig. 2. Scaling law of the ITER-type strand studied at 4.2 K, 12 T. Ic_{irr} symbols show data for which the n-value (between 10 and 100 μV/m) was decreased (beginning of irreversibility).

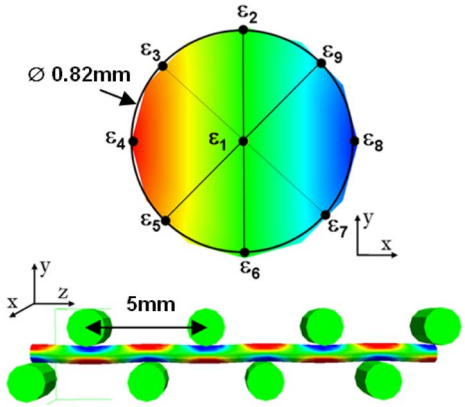

Fig. 3. MULTIFIL model of a strand in TARSIS.

conductors [5], and in this case to simulate the strain state of a single strand in the TARSIS experiment.

The code gives a detailed strain state of the strand for deflections ranging from 10 μm to 90 μm. Fig. 3 shows that the strain is calculated at 9 locations and is assumed to vary linearly in the cross-section.

B. Analysis of the Mechanical Model Results

Interesting features can be extracted from the strain maps calculated by MULTIFIL. The first one is the linearity of the maximum strain at the outer surface ($\varepsilon_{\mathrm{b\,max}}$) of the strands with the deflection. A linear fitting gives the following equation:

$$\varepsilon_{b\,\mathrm{max}} = 2.02 \times 10^{-2} \times D - 2.74 \times 10^{-2}$$

Where $\varepsilon_{\mathrm{b\,max}}$ is given at the filamentary radius of the strand in percentage, and D is the deflection in μm.

Knowing the twist pitch Lp of the filaments, it is then possible to calculate the strain map $\varepsilon(z)$ of any filament in the strand. Since the scaling law of the strand is known, one can associate a critical current map $I_{\mathrm{C}}(z)$ along each filament. Of course, this map is the result of the composition of the TARSIS sinusoidal load of period L_{T} and of the filament helical trajectory with twist pitch Lp.

IV. Electrical Limiting Cases

A. Definition

Analytical limiting cases have been proposed to evaluate simply the impact of bending on the critical current. Usually referred to as the "Ekin Models", they were used to describe

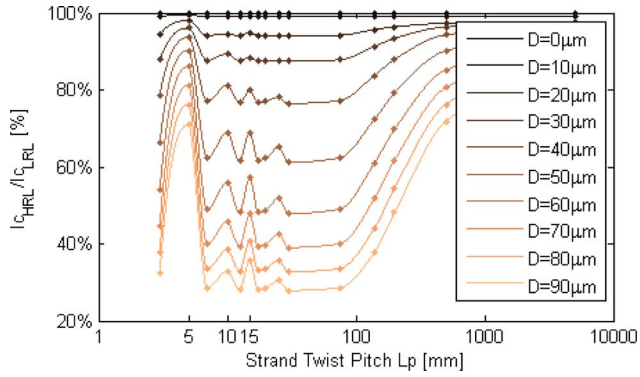

Fig. 4. Resonances peaks of the limiting cases critical currents ratio.

the "infinite bending" case ([6] and [7]). In this varying bending situation, they can still be used to apprehend extreme cases where the current either flows freely from one filament to its neighbors (Low Resistivity Limit: LRL) or is compelled to stay in the filament (High Resistivity Limit: HRL).

B. Strain Map Composition and Limiting Cases

It was shown in [8] that the twist pitch Lp and bending wavelength L_{T} composition into filaments strain maps can have a significant effect on the I_{C} value. This can be easily illustrated using the strain maps from MULTIFIL and the analytical limiting cases for all deflections. Indeed, in the LRL case, the filaments exchange current freely, therefore, the strand critical current I_{CLRL} is unaffected by this composition.

$$I_{C\ LRL} = (L)^{\frac{1}{n}} \left(\int_0^L \left(\frac{1}{I_C(z)} \right)^n dz \right)^{-1/n} \quad \text{with}$$

$$I_C(z) = \int_0^{2\pi} \int_0^{rzf} I_C(r,\theta,z)\, dr d\theta$$

But for the HRL case, each filaments individual critical current participates to the strand total I_{C}, if n is constant, by:

$$I_{C\ HRL} = \int_0^{2\pi} \int_0^{rzf} (L)^{\frac{1}{n}} \left(\int_0^L \left(\frac{1}{Ic(r,\theta,z)} \right)^n dz \right)^{-1/n} dr d\theta$$

Fig. 4 gives the ratio of the two limiting cases critical currents. A major resonant peak at $Lp = L_{\mathrm{T}}$ is visible for all deflections, just as in [8], as well as secondary peaks around 10 mm and 15 mm. This figure shows that, using only geometrical information with an adequate strain map, one can easily deduce the position of resonances between L_{T} and Lp.

V. CARMEN Electrical Model

A. Description

The CARMEN code is based on an electrical network with nodes connected by resistive or superconducting elements. It solves iteratively the non-linear problem of the superconducting

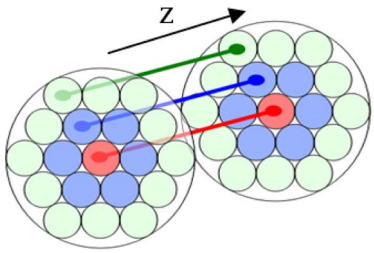

Fig. 5. CARMEN model of the strand with its 19 nodes per section and 19 superconducting elements in each longitudinal segment (only three visible).

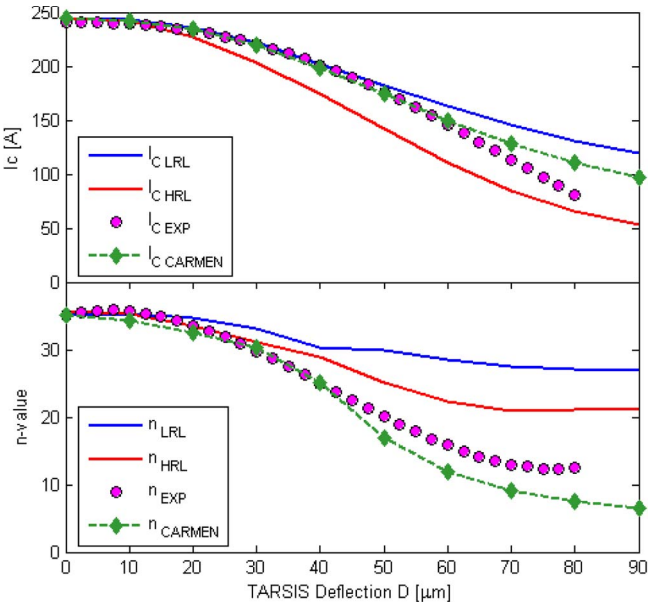

Fig. 6. Limiting cases, experiment, and CARMEN results for TARSIS experiment on TF strand.

elements resistivity and finds the currents in all the elements of the network [9]. For this calculation, it has been structured in a hexagonal network of 19 filaments.

Fig. 5 shows two cross-sections of the model connected by superconducting elements (only three in the figure for the sake of clarity).Each node is also connected to its first neighbors through a resistive link representing the matrix. The model has 50 longitudinal segments representing the 30 mm of strand modeled by MULTIFIL. The only free parameter in the model is the transverse resistances between elements in a cross-section. This value is found by the best fit of the $I_C(D)$ experimental curve.

B. Results and Comparison With Experiment

Fig. 6 (top plot) shows the best fit found for the experimental results. We can see that the simulation deviates from the experiment quite largely for a deflection above 75 μm. Above 60 μm, indeed, the strand is bent to strains above 1% for which it is most probable that filaments fracture reduce the current carrying capacity. Unfortunately, for the strand studied, there are no experimental data describing the irreversible behavior above 1% strain. Therefore, this effect was not modeled in this simulation.

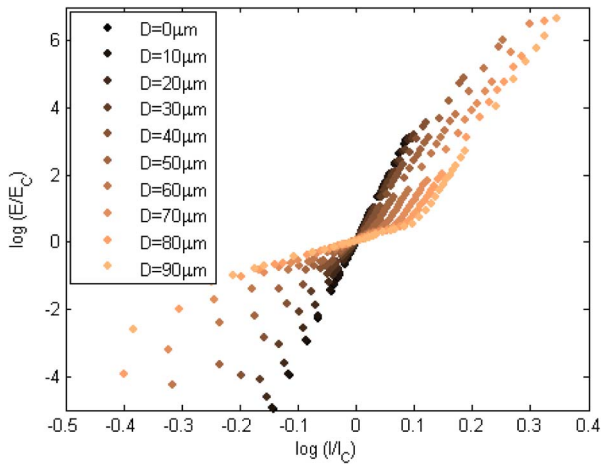

Fig. 7. LogLog plot of TARSIS $V(I)$ curves modeled by CARMEN.

The full V(I) curves can be plotted in loglog scale to see how the strand behaves at various electric fields.

Fig. 7 shows how the strand electric field is driven by the high n-values at either very high or at very low electric field, and how an intermediate behavior with low apparent n-value arises in the region of the critical electric field. The measure of n experimentally can thus be difficult, and depends on the electric field range chosen. Nevertheless, a comparison of measured and modeled n-values, here fitted over the 5 μV/m–70 μV/m range, can be made. Fig. 6 (bottom plot) presents these values along with the limiting cases n-values, which cannot be found analytically if we implement the $n(I_C)$ characteristic of this strand. Although the modeled n-value is not completely consistent with the experiment, it is still quite relevant up to 50 μm. For deflections above 50 μm, it is probable that filament breakage affects the V(I) curve and thus the n-value (as reported in [10]).

C. Extrapolation: TARSIS in Compression

For uniform bending, jacketed strands have been tested to see the influence of precompression on the performances. For periodic bending load, we can use the strand model previously "tuned" to extrapolate the strand behavior by adding a compressive strain relevant of the thermal precompression experienced by strands in ITER TF conductors. Here, a -0.45% strain, relevant of the jacket thermal compression during cooldown, was added to the whole strand strain map.

There are two interesting features in the plots of Fig. 8. First, it is quite obvious that if the experiment without compression shows a strand behaving mostly as a LRL composite, when changing the strain map (or the Ic distribution), it has an intermediate behavior with significant decrease of the ideal current distribution already around $D = 30$ μm. This is illustrated by the plots in Fig. 9 where the J_C maps extracted from MULTIFIL and the calculated current density maps from CARMEN are compared, for the two compressive cases, for 3 filaments in the model. It is clear on those plots that in the compressive case, even if the filaments have a current carrying capacity above that of the central filament, they are unable to transfer the current rapidly enough to exploit it. Therefore,

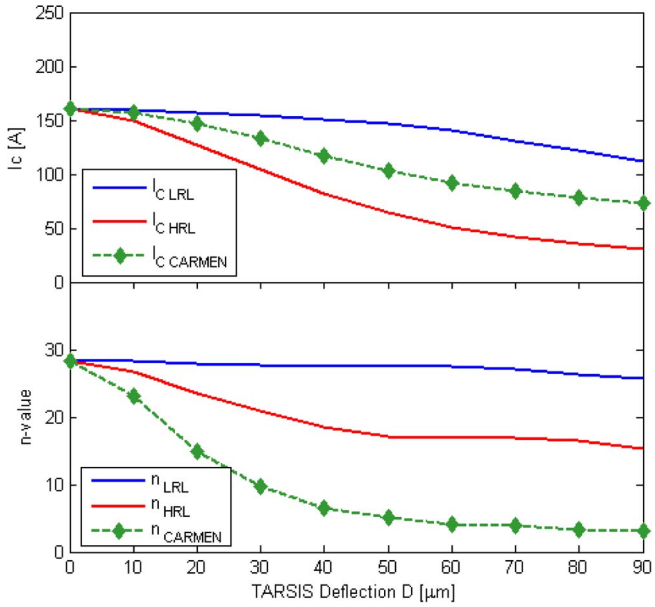

Fig. 8. Limiting cases and CARMEN results for a simulated TARSIS experiment with 0.45% compression.

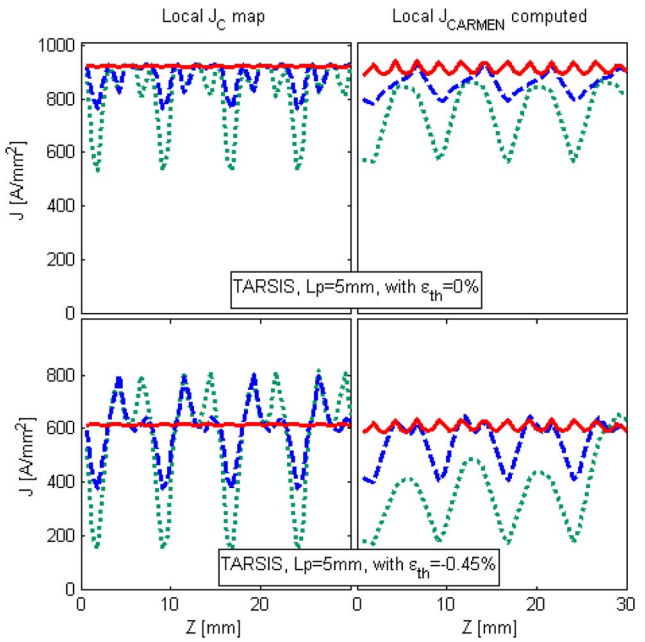

Fig. 9. Local J_{C} maps and current densities carried by three filaments in CARMEN in TARSIS, $Lp = 5$ mm (red is central, blue is first crown green is second crown filaments).

the LRL, which characterizes the possibility to use the whole superconducting surface in each section, is unreachable.

Second, the n-value decrease is far more pronounced in the case of a compressed strand, with values as low as 5 or 6 already at $D = 50$ μm. Therefore, it is clear that bending, in conjunction with axial compression, can be the source of single strand very low n-values. Indeed, bending strain relevant to real conductors can be evaluated around 0.5% to 0.6%. These values correspond to around 30 μm deflection for which, in the TARSIS experiment, the n-value is still around 30. In the "extrapolated" experiment, the n-value at that deflection

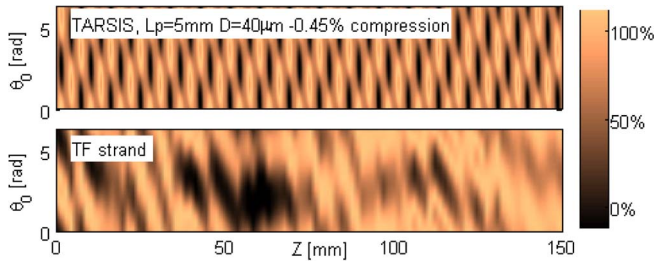

Fig. 10. $J_{\mathrm{C}}(\theta, z)$ maps at filamentary radius for TARSIS with compression and a TF strand cases.

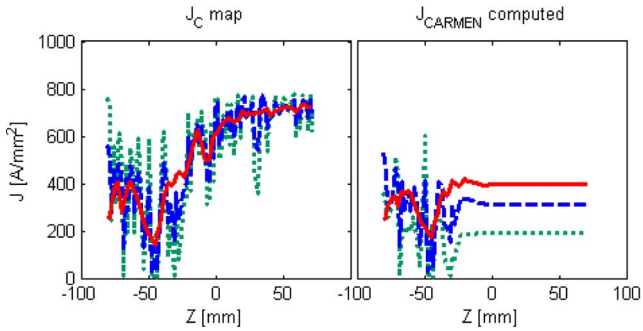

Fig. 11. J_{C} map and current density carried by three filaments in CARMEN for a TF strand (red is central, blue is first crown green is second crown filaments).

is around 10 which is much closer to experimental results on conductor samples tested in SULTAN.

D. Extrapolation: TF Strand

Of course, if the TARSIS experiment aims at producing a realistic periodic bending, the real strand loading in a CICC can be quite different. MULTIFIL has also produced strain maps for full TF petals. The loading applied to these sub-cables takes into account both the thermal compression ($\varepsilon_{\mathrm{th}} = -0.67\%$) and the Lorentz force at nominal current and field (0.84 N/mm). In order to compute the strand I_{C} map, a temperature of 6.25 K was assumed, and a background field comparable to the SULTAN field map in TF samples testing conditions was applied (10.78 T background field plus self-field due to 68 kA current).

Fig. 10 shows the resulting J_{C} map of the outer surface of the strand (at filamentary radius, for all initial angles θ_0) of one TF strand, (the volume distribution can be linearly deduced). These plots show that the J_{C} map, which results from the inhomogeneous strain and field maps applied, is highly irregular but with a spatial variation (both in Z and θ) far lower than that of TARSIS. Fig. 11 shows the local J_{C} map and the computed currents, by CARMEN, for 3 filaments of the same TF strand.

The computed currents emphasize that current redistribution is present in the lowest J_{C} areas, where electric field develops, but as soon as J_{C} rises, the currents are more or less constant. For all TF strands that were computed, the situation is similar, with a highly peaked electric field, in the region where both high strain and high magnetic field are present. That also implies that the strand is very close to the LRL limit, because of the long lengths available everywhere else to redistribute.

VI. Conclusion

In this article, the MULTIFIL mechanical model of the TARSIS experiment was presented and the resulting strain maps analyzed. These maps were used to compute J_C maps that served as input for the CARMEN electrical model of the strand. Using an ad hoc transverse resistivity value, we showed how TARSIS results could be reproduced, and how the model could serve as an extrapolation tool, providing useful insight of the strand behavior. The model showed that for a strand in compression, the TARSIS strain state would be very limiting (between LRL and HRL). For the a TF strand in a variable field map, however, only a limited length of strand is subject to high electric field, and thus large current redistribution, so that it is close to its LRL critical current. The next step will be to model mechanically and electrically larger conductors taking into account inter-strand exchange.

Acknowledgment

The authors would like to thank the ITER Conductor team for the support throughout this work. They thank all participants of the ITER Conductor Design Reconciliation Workshop for their fruitful and regular sharing of experience and results.

References

[1] D. Ciazynski, "Review of Nb3Sn conductors for ITER," *Fusion Eng. Des.*, vol. 82, no. 5–14, pp. 488–497, Oct. 2007.

[2] A. Devred, I. Backbier, D. Bessette, G. Bevillard, M. Gardner, M. Jewell, N. Mitchell, I. Pong, and A. Vostner, "Status of ITER development and production," *IEEE Trans Appl. Supercond.*, vol. 22, no. 3, p. 4 804 909, Jun. 2012.

[3] M. Breschi, A. Devred, M. Casali, D. Bessette, M. C. Jewell, N. Mitchell, I. Pong, A. Vostner, P. Bruzzone, B. Stepanov, T. Boutboul, N. Martovetsky, K. Kim, Y. Takahashi, V. Tronza, and W. Yu, "Results of the TF conductor performance qualification samples for the ITER project," *Supercond. Sci. Technol.*, vol. 25, no. 9, p. 095004, Sep. 2012.

[4] A. Nijhuis, N. C. van den Eijnden, Y. Ilyin, E. G. van Putten, G. J. T. Veening, W. A. J. Wessel, A. den Ouden, and H. H. J. ten Kate, "Impact of spatial periodic bending and load cycling on the critical current of a Nb3Sn strand," *Supercond. Sci. Technol.*, vol. 18, no. 12, pp. S273–S283, Dec. 2005.

[5] H. Bajas, "Numerical simulation of the mechanical behavior of the ITER cable-in-conduit conductors," Ph.D. dissertation, Ecole Centrale de Paris, Chatenay-Malabry, France, Mar. 14, 2011.

[6] J. W. Ekin, "Current transfer in multifilamentary superconductors I. Theory," *J. Appl. Phys.*, vol. 49, no. 6, pp. 3406–3409, Jun. 1978.

[7] D. Ciazynski and A. Torre, "Analytical formulae for computing the critical current of an Nb_3Sn strand under bending," *Supercond. Sci. Technol.*, vol. 23, no. 12, p. 125 005, Dec. 2010.

[8] Y. Miyoshi, C. Zhou, E. P. A. van Lanen, M. M. J. Dhallé, and A. Nijhuis, "Modelling of current distribution in Nb_3Sn multifilamentary strands subjected to bending," *Supercond. Sci. Technol.*, vol. 25, no. 5, p. 054003, May 2012.

[9] A. Torre, H. Bajas, D. Ciazynski, D. Durville, and K. Weiss, "Mechanical-electrical modeling of stretching experiment on 45 Nb3Sn strands CICCs," *IEEE Trans. Appl. Supercond.*, vol. 21, no. 3, pp. 2042–2045, Jun. 2011.

[10] B. Seeber, G. Mondonico, and C. Senatore, "Toward a standard for critical current versus axial strain measurements of Nb_3Sn," *Supercond. Sci. Technol.*, vol. 25, no. 5, p. 054002, May 2012.

[11] L. Muzzi, A. della Corte, A. Di Zenobio, S. Turtu, L. Zani, G. Samuelli, E. Salpietro, and A. Vostner, "Pure bending strain experiments on jacketed Nb_3Sn strands for ITER," *IEEE Trans. Appl. Supercond.*, vol. 17, no. 2, pp. 2591–2594, Jun. 2007.